Journal of Photochemistry, 13 (1980) 21 - 33

PICOSECOND TIME RESOLUTION BY A CONTINUOUS WAVE LASER AMPLITUDE MODULATION TECHNIQUE I: A CRITICAL INVESTIGATION

HEINRICH GUGGER and GION CALZAFERRI

Institute for Inorganic and Physical Chemistry, University of Bern, Freiestrasse 3, Bern (Switzerland)

(Received September 17, 1979)

Summary

A continuous wave laser technique for picosecond lifetime measurements is presented which takes advantage of phase relations between two amplitude-modulated light beams travelling on different optical paths. Two determinations of such a phase (Φ_0 and Φ_1) yield a phase shift Φ_τ ($= \Phi_1 - \Phi_0$) which can be related to the lifetime of the sample. We stress the importance of a critical error estimation. A detailed analysis of error sources and their consequences is performed. Favourable measurement parameters can be obtained from the error discussion. The result is very encouraging since the accuracy can be tuned to the low picosecond range. The resolution limit is set by the dynamic calibration of the spectrum analyser.

1. Introduction

1.1. Objective

Measurements of molecular decays on the picosecond time scale [1] require careful control of the experimental parameters since there are a series of hidden traps. Although the results may be reproducible to within a few picoseconds, this is no proof of absolute accuracy. Reliable results must be based on a macroscopic check-out of the method against well-defined physical parameters. The experiment should allow closely spaced multiexponential decays to be analysed [2, 3]; otherwise misleading interpretation detracts from absolute accuracy. When a photomultiplier is used as the detector, the time response of the tube must be calibrated against spectral response. Because of the wavelength-dependent kinetic energy of the electrons emitted from the photocathode, different spectral light distributions cause transit time lags and subsequent lifetime errors up to some hundreds of picoseconds depending on the tube type. This phenomenon is especially important for luminescent samples with a significant Stokes's

shift [4]. The signal-to-noise ratio must also be considered, since coherent noise is generated at the measurement frequency in modulation experiments.

Modulation techniques have some advantages over pulse measurements which are subject to the following problems.

(1) Excessive power density may cause optical and chemical nonlinearities as well as unwanted secondary processes.

(2) The real time observation of picosecond phenomena shifts electronic acquisition to the gigahertz region with some high frequency difficulties.

(3) The error estimation becomes cumbersome since it is difficult to separate and to determine definitely the rates of the error parameters.

The basic idea of working with modulated light is not new in luminescence spectroscopy and possible applications for picosecond lifetime measurements have appeared in the literature [5 - 7]. However, no critical analysis of the picosecond accuracy obtained has so far been published.

1.2. The method

A luminescent sample is excited by a quasi-monochromatic amplitude-modulated continuous wave (CW) laser beam. We introduce a general light-forcing function denoted by $F(t)$. Provided that the system response is linear, the emission function $E(t)$ is given by the convolution product of $F(t)$ and the transfer function $T(t)$ which is characteristic of the sample under study.

$$E(t) = F(t)*T(t) = \int_{-\infty}^{+\infty} F(t')T(t-t')\mathrm{d}t' \qquad (1)$$

Figure 1 illustrates the case where $F(t)$ is sinusoidal and $T(t)$ is a single exponential decay with a decay constant τ. The resulting emission function is shifted in phase relative to the forcing function. Furthermore its amplitude is significantly compressed and depends on the actual $\omega\tau$ configuration. This work deals solely with the accurate determination of the phase shift.

For a single exponential decay this phase shift Φ_τ can be related to the decay time τ of the luminescent sample by [8]

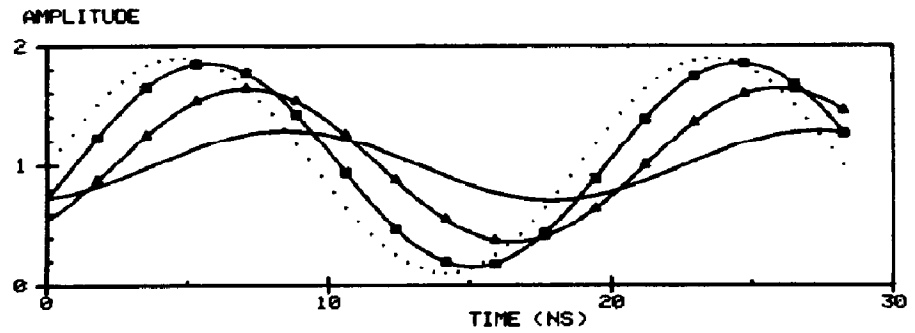

Fig. 1. Time–domain plots of the emission function (the modulation frequency ν (= $\omega/2\pi$) is fixed at 53.0517 MHz, whereas the decay time constant τ is varied): ···, light-forcing function or τ = 0; ■, τ = 1 ns ($\omega\tau$ = 1/3); ▲, τ = 3 ns ($\omega\tau$ =1); ——, τ = 9 ns ($\omega\tau$ = 3).

$$\tau = \frac{1}{\omega} \tan \Phi_\tau \qquad (2)$$

A detailed description of the apparatus will be given in a forthcoming publication [9]. A schematic diagram of the experimental set-up for the following error discussion is given in Fig. 2.

The modulated beam is split up. The transmitted beam enters the sample chamber where it hits the scattering medium or, in the second measurement when the scatterer has been replaced by the sample, where it excites the sample. For both cases the reflected part at the beam splitter serves as a phase reference and is fed via an optical delay line into the reference housing. The light generated in the two chambers is individually collected, is homogeneously mixed in optical fibres and is directed onto the photomultiplier cathode. The anode of the photomultiplier is connected to the input of the spectrum analyser from where the a.c. data acquired is transferred to a minicomputer.

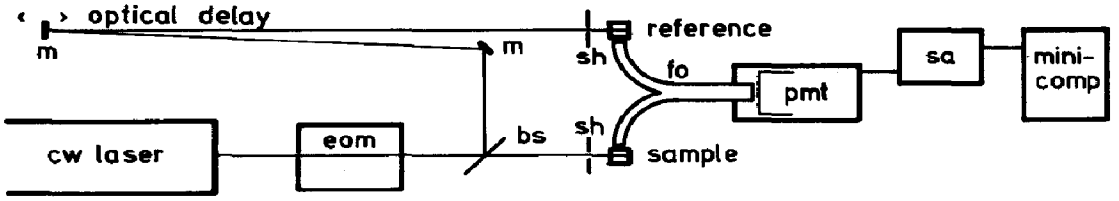

Fig. 2. A schematic diagram of the experimental set-up: bs, beam splitter; m, mirror; eom, electro-optic modulator; pmt, photomultiplier; fo, fibre optics; sa, spectrum analyser; sh, shutter.

1.3. Acquisition cycles

To evaluate τ we require the following two measurements of Φ: Φ_0, where both chambers contain identical scattering media, to set a "phase null"; Φ_1, where the sample replaces the scatterer in the sample chamber. The difference $\Phi_\tau (= \Phi_1 - \Phi_0)$ represents the phase shift caused by the lifetime of the sample and yields the data required for the τ calculus.

The determination of $\Phi_i (i = 0, 1)$ is a four-step procedure involving the measurement of (1) the reference level $R(t)$, (2) the sample level $S(t)$, (3) the sum signal level $B(t)$ and (4) the noise level $N(t)$. From the information $R(t)$, $S(t)$ and $B(t)$ Φ_i can be calculated and the noise level $N(t)$ appears only in the error estimation.

2. Evaluation of τ for single exponential decay

By superimposing the reference beam intensity

$$R(t) = R_0 \exp (i\omega t)$$

and the light intensity emitted by the sample

$$S(t) = S_0 \exp\{i(\omega t + \Phi)\}$$

on the photomultiplier cathode, we obtain the sum signal intensity

$$B(t) = R(t) + S(t)$$
$$= B_0(\Phi) \exp\{i(\omega t + \Phi')\}$$
$$B_0^2(\Phi) = R_0^2 + S_0^2 + 2R_0S_0 \cos\Phi$$

The solution for Φ is given by

$$\Phi = \arccos\left(\frac{B_0^2(\Phi) - R_0^2 - S_0^2}{2R_0S_0}\right) \tag{3}$$

From the spectrum analyser the values X_R, X_S, X_B and X_N in units of dBm are obtained during cycles of the four-step procedure described in Section 1.3. These values are related to the light intensities by

$$R_0^2 = 10^{X_R/10} \qquad S_0^2 = 10^{X_S/10} \qquad B_0^2 = 10^{X_B/10} \qquad N_0^2 = 10^{X_N/10} \tag{4}$$

Equation (3) can therefore be written as

$$\Phi = \arccos\left(\frac{10^{X_B/10} - 10^{X_R/10} - 10^{X_S/10}}{2 \times 10^{(X_R + X_S)/20}}\right) \tag{5}$$

For practical reasons we introduce the following substitutions:

$$\alpha \equiv (X_R - X_S)/20 \qquad \beta \equiv (X_B - X_S)/10 \qquad \gamma \equiv (X_N - X_B)/10 \tag{6}$$

This is shown graphically in Fig. 3. Hence the argument of the arccos function eqn. (5) simplifies to

$$E(\alpha, \beta) \equiv 0.5 \times 10^{-\alpha}(10^{\beta} - 10^{2\alpha} - 1) \tag{7}$$

and eqn. (5) can be written as

$$\Phi_i = \arccos\{E(\alpha_i, \beta_i)\} \qquad i = 0, 1 \tag{8}$$

α and β now become the crucial measurement parameters in units of fractions of decibels. γ will appear only in the error calculation.

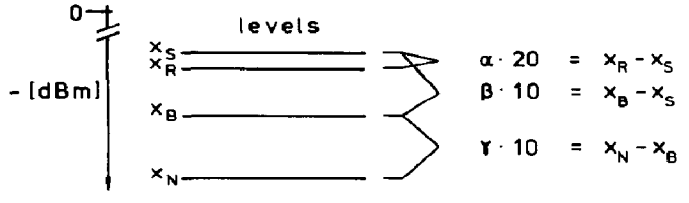

Fig. 3. The acquisition levels and arithmetic substitutions.

3. Error handling

In modulation luminescence decay measurements two categories of errors appear.

(1) Errors imposed by instrumental limitations which can be treated mathematically.

(2) Systematic errors caused by the design and/or the nature of the experiment. This type of error can only be eliminated by meticulous care in experimentation. Special attention has to be paid to the following points.

(a) The delayed time response of photomultipliers for photons of wavelength longer than the excitation light introduces a new, though stable, phase shift Φ_1 and therefore simulates a false decay time. Symmetry reasons render a purely mathematical elimination impossible. A suggestion for solving this problem will be discussed in another publication [3].

(b) Geometrical aspects such as the illuminated "target" shape congruence, the identity of the light collection paths and the cathode region where the guided light is detected should be considered [9].

(c) Optical components which are replaced (filters, attenuators and delay length alteration) must be carefully checked for spurious retardation caused by different refractive indices. Astonishingly good reproducibility can be attained by the minimization of type (1) errors. Truly reliable data with an absolute accuracy of several picoseconds can, however, only be obtained if the set-up has been checked within the limits of type (1) errors against errors of type (2).

3.1. Errors of type (1)

Starting with eqn. (2) the error in τ can be expressed as

$$d\tau = \left(\frac{\partial\tau}{\partial\omega}\right)_\Phi d\omega + \left(\frac{\partial\tau}{\partial\Phi}\right)_\omega d\Phi_\tau \tag{9}$$

where $d\omega$ depends on electronic stability specifications and $d\Phi_\tau$ is composed of $d\Phi_E$ and $d\Phi_\gamma$.

$$d\Phi_E = \frac{d\Phi}{dE} dE$$

$$dE = \left(\frac{\partial E}{\partial\alpha}\right)_\beta d\alpha + \left(\frac{\partial E}{\partial\beta}\right)_\alpha d\beta$$

and $d\Phi_\gamma$ is the contribution to the error in Φ_i caused by the signal-to-noise ratio. Assuming a gaussian distribution, we can write the following equation for the error in τ:

$$d\tau = \left[\left\{\left(\frac{\partial\tau}{\partial\omega}\right)_\Phi d\omega\right\}^2 + \left\{\left(\frac{\partial\tau}{\partial\Phi}\right)_\omega \left(\frac{d\Phi}{dE}\right)\left(\frac{\partial E}{\partial\alpha}\right)_\beta d\alpha\right\}^2 + \right.$$

$$\left. + \left\{\left(\frac{\partial\tau}{\partial\Phi}\right)_\omega \left(\frac{d\Phi}{dE}\right)\left(\frac{\partial E}{\partial\beta}\right)_\alpha d\beta\right\}^2 + \left\{\left(\frac{\partial\tau}{\partial\Phi}\right)_\omega d\Phi_\gamma\right\}^2\right]^{1/2} \tag{10}$$

The individual differentials can be evaluated:

$$\left(\frac{\partial\tau}{\partial\omega}\right)_\Phi = \frac{1}{\omega^2}\left(-\tan\Phi + \frac{\omega}{\cos^2\Phi}\frac{\partial\Phi}{\partial\omega}\right) = \frac{1}{\omega^2}\left(-\tan\Phi + \frac{\Phi}{\cos^2\Phi}\right)$$

$$\left(\frac{\partial \tau}{\partial \Phi}\right)_{\omega} = \frac{1}{\omega \cos^2 \Phi}$$

$$\left(\frac{d\Phi}{dE}\right) = \frac{-1}{(1 - E^2)^{1/2}}$$

$$\left(\frac{\partial E}{\partial \alpha}\right)_{\beta} = -(E + 10^{\alpha}) \ln 10$$

$$\left(\frac{\partial E}{\partial \beta}\right)_{\alpha} = 0.5 \times 10^{\beta - \alpha} \ln 10$$

$d\omega$ and $d\beta$ depend on the acquisition electronics and $d\alpha$ is the root mean square (r.m.s.) error of acquired levels of X_S and X_R. The differential $d\Phi_\gamma$ cannot be evaluated directly and must be discussed in some more detail.

In this context it should be mentioned that the term "noise" denotes radiation scatter at the modulation frequency generated by the power circuits of the modulator and picked up by the detection electronics. It is definitely not a "white noise"; therefore it is reasonable to assign an amplitude and a phase to this composite non-statistical signal.

Because its phase cannot be fixed in the experiment, it is necessary to integrate the resulting errors $d\Phi_\gamma$ over all relative noise phases of a full period to obtain the mean error contribution $\langle d\Phi_\gamma \rangle$. Another important physical implementation is the fact that this noise superimposes only on the signal in electronic circuits and not in the optical part of the experiment. Thus noise adds to sample, reference and sum signals; the latter, however, is the sum of two noise-free origins, since the mixing is performed optically.

To calculate the error $d\Phi_\gamma$ we proceed in the following way. The sample beam is set as a phase standard with $\Phi_S = 0$. The noise-free reference beam is then shifted by Φ_R and the noise by ϕ_N. We calculate ϕ_R which denotes the phase of the reference beam under the influence of noise. The difference between the "noisy" and the noise-free reference phase, given by $d\Phi_\gamma = |\Phi_R - \phi_R|$, determines the amount of the phase error due to the signal-to-noise ratio.

In a first step we add noise to the original signals $R(t)$, $S(t)$ and $B(t)$:

$$N(t) = N_0 \exp\{i(\omega t + \phi_N)\}$$

$$S'(t) = \exp(i\omega t)\{S_0 + N_0 \exp(i\phi_N)\}$$

$$R'(t) = \exp(i\omega t)\{R_0 \exp(i\phi_R) + N_0 \exp(i\phi_N)\}$$

$$B'(t) = \exp(i\omega t)\{R_0 \exp(i\phi_R) + S_0 + N_0 \exp(i\phi_N)\}$$

Similar to eqn. (4) we form

$$I_{R'} = 10^{X_{R'}/10}$$
$$= R'(t)R'^{*}(t)$$

and $I_{S'}$ and $I_{B'}$ are formed analogously. The substitution $\bar{\phi} = \phi_R - \phi_N$ leads to

$$\begin{aligned} I_{R'} &= R_0^2 + N_0^2 + 2R_0N_0 \cos\bar{\phi} \\ I_{S'} &= S_0^2 + N_0^2 + 2S_0N_0 \cos\phi_N \\ I_{B'} &= R_0^2 + S_0^2 + N_0^2 + 2R_0S_0 \cos\phi_R + 2R_0N_0 \cos\bar{\phi} + 2S_0N_0 \cos\phi_N \end{aligned} \tag{11}$$

With the substitution of eqns. (6) for $X_{R'}$, $X_{S'}$, $X_{B'}$ and X_N the variable γ can be introduced:

$$\begin{aligned} I_{R'} &= 10^{(2\alpha-\beta-\gamma+X_N/10)} \\ I_{S'} &= 10^{(-\beta-\gamma+X_N/10)} \\ I_{B'} &= 10^{(-\gamma+X_N/10)} \end{aligned} \tag{12}$$

From eqns. (11)

$$I_{B'} = I_{S'} + I_{R'} - N_0^2 + 2R_0S_0 \cos\phi_R$$

Together with eqns. (12) $\cos\phi_R$ is given by

$$\cos\phi_R = \frac{10^{(-\gamma+X_N/10)} - 10^{(-\beta-\gamma+X_N/10)} - 10^{(2\alpha-\beta-\gamma+X_N/10)} + 10^{X_N/10}}{2R_0S_0} \tag{13}$$

This formula is very similar to eqn. (3), but the denominator cannot be incorporated straightforwardly into our substitutions and R_0 and S_0 have to be calculated from eqns. (11):

$$\begin{aligned} R_0 &= 10^{X_N/20}\{-\cos\bar{\phi} + (10^{2\alpha-\beta-\gamma} - \sin^2\bar{\phi})^{1/2}\} \\ S_0 &= 10^{X_N/20}[-\cos(\phi_R - \bar{\phi}) + \{10^{-\beta-\gamma} - \sin^2(\phi_R - \bar{\phi})\}^{1/2}] \end{aligned} \tag{14}$$

Substitution of eqns. (14) into eqn. (13) leaves us with the final equation

$$\cos\phi_R = \frac{10^{-\gamma} - 10^{-\beta-\gamma} - 10^{2\alpha-\beta-\gamma} + 1}{2\{-\cos\bar{\phi} + (10^{2\alpha-\beta-\gamma} - \sin^2\bar{\phi})^{1/2}\}[-\cos(\phi_R - \bar{\phi}) + \{10^{-\beta-\gamma} - \sin^2(\phi_R - \bar{\phi})\}^{1/2}]} \tag{15}$$

The argument $X_N/10$ has vanished. This means that ϕ_R does not depend on the absolute noise level but only on the signal-to-noise ratio.

Equation (15) is an implicit function for ϕ_R and can only be solved iteratively [10]. We introduce the following substitutions:

$$C = 10^{-\gamma} - 10^{-\beta-\gamma} - 10^{2\alpha-\beta-\gamma} + 1$$

$$u(\bar{\phi}) = -\cos\bar{\phi} + (10^{2\alpha-\beta-\gamma} - \sin^2\bar{\phi})^{1/2}$$

$$v(\phi_R, \bar{\phi}) = -\cos(\phi_R - \bar{\phi}) + \{10^{-\beta-\gamma} - \sin^2(\phi_R - \bar{\phi})\}^{1/2}$$

$$y(\phi_R) = -2\cos\phi_R$$

$$z(\phi_R, \bar{\phi}) = uv$$

leading to

$$f(\phi_R, \bar{\phi}) = 0$$
$$= C + y(\phi_R)z(\phi_R, \bar{\phi}) \tag{16}$$

Values for ϕ_R are calculated by iteration with fixed $\bar{\phi}$ to satisfy eqn. (16). The Taylor expansion is applied:

$$(\phi_R^{i+1})_{\bar{\phi}} = (\phi_R^i)_{\bar{\phi}} - f(\phi_R^i)_{\bar{\phi}} \left\{\left(\frac{\partial f}{\partial \phi_R}(\phi_R^i)\right)_{\bar{\phi}}\right\}^{-1}$$

with the differentials

$$\left(\frac{\partial f}{\partial \phi_R}\right)_{\bar{\phi}} = z\left(\frac{\partial y}{\partial \phi_R}\right) + y\left(\frac{\partial z}{\partial \phi_R}\right)_{\bar{\phi}} \tag{17}$$

$$\left(\frac{\partial z}{\partial \phi_R}\right)_{\bar{\phi}} = v\left(\frac{\partial u}{\partial \phi_R}\right) + u\left(\frac{\partial v}{\partial \phi_R}\right)_{\bar{\phi}} \tag{18}$$

Since $\partial u/\partial\phi_R = 0$, eqn. (17) reduces to

$$\left(\frac{\partial f}{\partial \phi_R}\right)_{\bar{\phi}} = z\left(\frac{\partial y}{\partial \phi_R}\right) + yu\left(\frac{\partial v}{\partial \phi_R}\right)_{\bar{\phi}} \tag{19}$$

with

$$\left(\frac{\partial v}{\partial \phi_R}\right)_{\bar{\phi}} = \sin(\phi_R - \bar{\phi}) - \frac{\sin\{2(\phi_R - \bar{\phi})\}}{2\{10^{-\beta-\gamma} - \sin^2(\phi_R - \bar{\phi})\}^{1/2}} \tag{20}$$

Figure 4(b) shows the dependence of $d\phi_\gamma$ on the relative phase $\bar{\phi}$. For good experimental parameter settings (high signal-to-noise ratio, $\alpha = 0$, $-\beta$ large) the function is very similar to a sine function. This means that ϕ_R oscillates around Φ_R. Under worse experimental conditions (low signal-to-noise ratio, $\alpha \neq 0$, small β) the symmetry deteriorates but preserves periodicity with 2π. To obtain the average error contribution and to avoid assigning a fixed phase to the noise, we have to intergrate over one whole period of $\bar{\phi}$:

$$\langle d\phi_\gamma \rangle = \frac{1}{2\pi}\int_0^{2\pi} |d\phi_\gamma|\, d\bar{\phi} \tag{21}$$

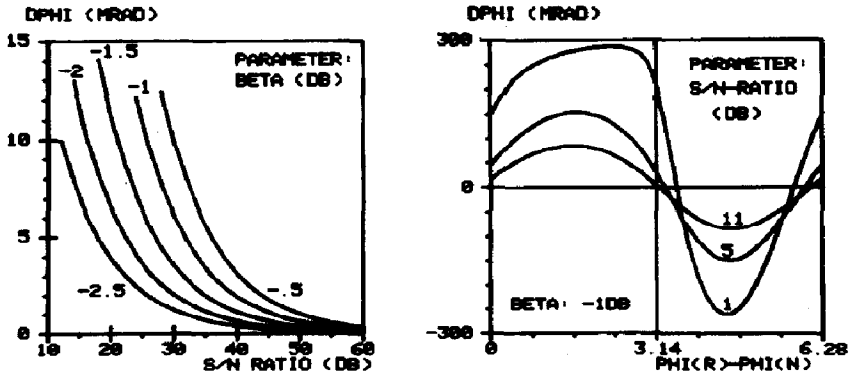

Fig. 4. The phase error caused by noise (DPHI ≡ $d\Phi_\gamma$): (a) $d\Phi_\gamma$ *vs.* the signal-to-noise ratio ($\beta \equiv$ BETA); (b) $d\Phi_\gamma$ *vs.* $\bar{\phi} = \phi_R - \phi_N$ (≡ PHI (R) — PHI (N)). Loss in symmetry is emphasized by choosing extremely bad experimental conditions.

4. Error discussion

Knowledge of these type (1) errors in analytical form allows the parameter ranges to be searched to find optimum experimental conditions. According to eqn. (9) the time error $d\tau(\omega, \Phi)$ can be split into a phase term $d\Phi_\tau$ and a frequency term $d\omega$. We will first discuss the parameters governing the total phase error $d\Phi_\tau$.

4.1. The spectrum analyser specifications as accuracy limits

The dynamic amplitude calibration of the screen differs depending on the type of spectrum analyser used. Our set-up [9] with the Tektronix 7L13 analyser and the Tektronix TR501 tracking generator acquires signal levels within the following absolute limits:

±1	dB in the dynamic range	5 - 14 dB	$(-0.5 \geqslant \beta \geqslant -1.4)$
±1.5	dB in the dynamic range	15 - 70 dB	$(-1.5 \geqslant \beta \geqslant -7)$

The r.m.s. error of an averaged level determination (approximately 16 000 samples) takes a value of about 5×10^{-3} dB. Thus the relative errors $d\alpha'$, and $d\beta'$ in α and β are

$$d\alpha' \approx 5 \times 10^{-4}\,\text{dB}$$

$$d\beta' \approx 1 \times 10^{-3}\,\text{dB}$$

It can be derived from Figs. 5 and 6 that α should be tuned to zero. This means that the error contribution from the screen calibration can be neglected and the relative error equals the absolute. The same is, however, not true for β. In this case we are forced to use the calibration value which depends on the dynamic range used and $d\beta'$ can be neglected. The combination TR501–7L13 together with a Tektronix 7D14 counter scales the frequency accuracy down to 10 Hz. It is therefore reasonable to vary the experimental errors of the parameters α, β and ω within the following ranges:

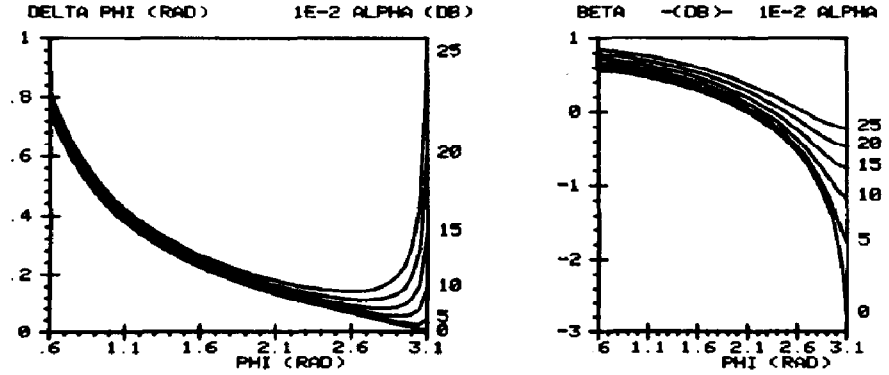

Fig. 5. (a) The phase shift error $d\Phi_E$ (≡ DPHI) and (b) the damping parameter β (≡ BETA) as functions of the phase Φ_i (≡ PHI). The parameter α (≡ ALPHA) is the measure for equalization of the levels X_R and X_S.

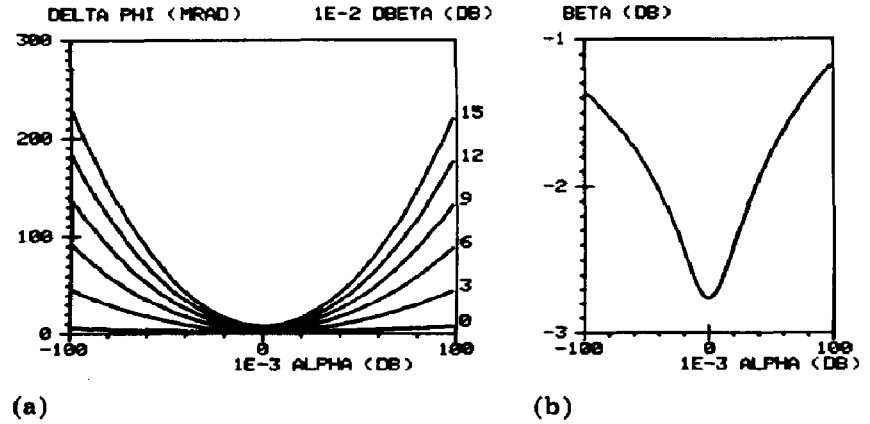

Fig. 6. (a) The phase shift error $d\Phi_E$ (≡ DPHI) and (b) the damping measure β (≡ BETA) as functions of the equalization α (≡ ALPHA) at a phase Φ_i of 3.1 rad. The parameter $d\beta$ (≡ DBETA) is the error in β.

$$d\alpha = 5 \times 10^{-4}\,\text{dB}$$

$$d\beta = 0 - 0.15\,\text{dB}$$

$$d\omega = 100\,\text{Hz}$$

4.2. The optimum range for Φ_i

As defined in Section 1, Φ_τ is the difference between Φ_1 and Φ_0. In this experiment the error in Φ_i (i = 0,1) varies enormously depending on the absolute values of Φ_i. It follows from Fig. 5 that $d\Phi_E$ decreases with increasing phase. The best results are obtained in the range $\Phi \approx \pi$ where $\beta_{(\alpha=0)}$ is maximal. It should be noted that the error function $d\Phi_E$ is symmetric with respect to π. In order to obtain the highest precision for both determinations, it is necessary to set the macroscopic phase shifter (the optical delay line)

to such a length that $\Phi_0 \approx \pi + \Phi_\tau/2$ and $\Phi_1 \approx \pi - \Phi_\tau/2$. Figure 6 shows that $d\Phi_E$ is minimal for $\alpha = 0$ at a fixed phase shift Φ_i. It can be seen that $d\beta$ has a larger effect on $d\Phi_E$ when α assumes values away from zero. The effect is less dramatic, however, when Φ_i is not as close to π as in the plot presented.

In summary, two beams (sample and reference) perfectly adjusted for equal modulation depth but dephased by $\pi \pm \Phi_\tau/2$ with $\Phi_\tau \ll \pi$ represent the optimum measurement configuration with respect to the parameters α and β.

4.3. Noise analysis results

By variation of parameters in calculations of the kind presented, it can be shown that the phase error in the region very close to $\Phi_i = \pi$ is sensitive to non-ideal measurement parameters. Noise analysis even now prohibits $\Phi_i = \pi$. Since the levels X_B and X_N coincide, the signal-to-noise ratio becomes zero. The maximum tolerable $d\Phi_\gamma$ allows the minimum signal-to-noise ratio to be deduced, according to Fig. 4(a), in relation to the known $d\Phi_E$. Reasonable measurements require signal-to-noise ratios in the range 30 - 50 dB (*i.e.* $-5 < \gamma < -3$). It follows from Figs. 5 and 6 that a slight deviation from $\Phi_i = \pi$ satisfies this requirement because of the steepness of the β function.

4.4. Time error $d\tau(\omega, \Phi)$

Electronic components currently in use [9] provide a frequency stability and accuracy which keep the error contribution caused by uncertainties in ω to a level of some 10^{-15} s. The phase error effect is larger by a factor of 10^3.

Figure 7 shows the dependence of $d\tau$ on the modulation frequency, the parameter being $d\Phi_\tau = \{(d\Phi_0)^2 + (d\Phi_1)^2\}^{1/2}$. The resulting errors are linear with respect to $d\Phi_\tau$, but not with respect to the frequency. It is obvious that $d\tau$ decreases with higher modulation frequencies for a fixed decay time. But at the same time the emission function eqn. (1) suffers a loss in modulation depth (Fig. 1), causing experimental problems (noise and photomultiplier saturation [9]).

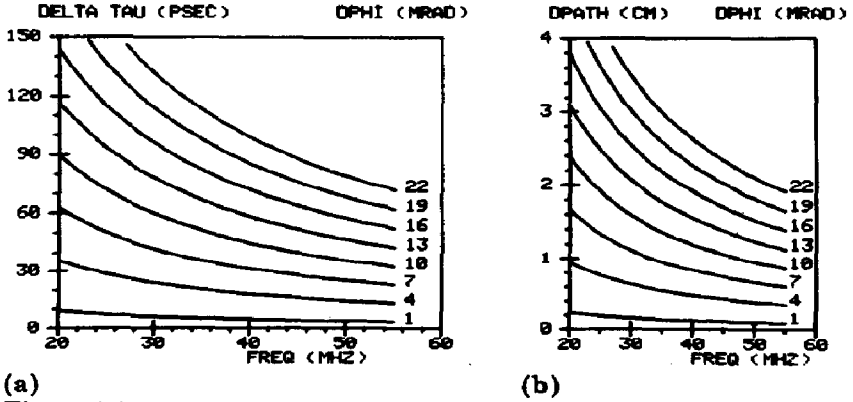

(a) (b)

Fig. 7. (a) The resulting time error $d\tau$ (≡ DELTA TAU) and (b) the error in the optical path length determination (≡ DPATH) *vs.* the modulation frequency at a phase Φ_i of 2.8 rad. The parameter $d\Phi_\tau$ (≡ DPHI) is the total shift error.

Furthermore, the path length error $\Delta L = d\Phi(c/\omega)$ of the optical delay path length arising from the phase error $d\Phi$ can be found from Fig. 7. (The velocity of light is denoted by c.) This conversion of the phase into a path length provides us with the possibility of calibrating our experimental set-up. The end mirror of the delay line is positioned at an exactly measured path length difference between the sample and reference beam. Identical scatterers are placed in both housings. To perform the system check-out described in Section 1 we determine Φ_0 at various frequencies. The path lengths, resulting from subsequent Φ_0-to-L conversion, have to equal the path length measured physically within the limits of the error estimation presented. Only the successful performance of this check-out allows further systematic errors of type (2) (defined in Section 3) to be excluded. Most other modulation techniques lack this possibility and use chemical solutions with known decay lifetimes as standards.

5. Conclusions

The analysis presented in this work helps to reveal the possible accuracy in relation to the apparatus and technique applied. Our modulation technique is especially interesting for short time analysis ($\leq$ 1 ns), since the relative error $d\tau/\tau$ decreases slightly with faster decay times of the sample under study. The accuracy is flexible owing to the experimental freedom provided by the manner in which the optical delay line is used. It depends markedly on the refinements of the electronic equipment. Menzel and Popovic [5] have carried out a similar experiment concerning the set-up. However, it is more fascinating for its simplicity and "low costs" than for the published accuracy which is too optimistic.

The decisive contribution to the total error turns out to be the phase shift error $d\Phi_\tau$, whereas the error arising from the modulation frequency uncertainty can be neglected in our set-up. $d\Phi_\tau$ is made up of two parts. The first is $d\Phi_E$ which includes errors inherent in the acquisition procedure. The spectrum analyser as a frequency selective level meter limits the resolution by its dynamic range calibration. The second part of $d\Phi_\tau$ is $d\Phi_\gamma$ which includes effects of the coherent non-statistical noise. It is shown that a minimal signal-to-noise ratio of about 30 - 40 dB should be maintained.

Moreover, the error analysis serves as a valuable guide when choosing settings of the experimental parameters. In this respect perfectly equalized sample and reference levels, as well as a large damping of the sum level, provide the best accuracy.

Acknowledgments

We thank Professor Dr. E. Schumacher for his support and Dr. S. Leutwyler for providing us with his laser knowledge and skill. Both helped

us in many critical and constructive discussions. We also thank J. Baumann for his contributions to the signal-to-noise ratio calculations. This work was supported by the Swiss National Science Foundation (Grant No. 2.919-0.77).

References

1 C. V. Shank, E. P. Ippen and S. L. Shapiro, *Picosecond Phenomena*, Springer, Berlin, 1978.
2 I. M. Warner, G. D. Christian, E. R. Davidson and J. B. Callis, *Anal. Chem.*, *49* (1977) 564.
R. D. Spencer and G. Weber, *Ann. N.Y. Acad. Sci.*, *58* (1968) 361.
3 H. Gugger, *Doctoral Thesis*, University of Bern, Switzerland, 1980.
4 R. K. Bauer and A. Balter, *Opt. Commun.*, *28* (1979) 91, and references cited therein.
5 A. Müller, R. Lumry and H. Kokobun, *Rev. Sci. Instrum.*, *36* (1965) 1214.
K. Schurer, P. G. Ploegaert and P. C. M. Wennekes, *J. Phys. E*, *9* (1976) 821, and references cited therein.
E. R. Menzel and Z. D. Popovic, *Chem. Phys. Lett.*, *45* (1977) 537.
E. R. Menzel and Z. D. Popovic, *Rev. Sci. Instrum.*, *49* (1978) 39.
6 H. Gugger, S. Leutwyler, E. Schumacher and G. Calzaferri, Kurzzeitmessungen mit Hilfe von CW-Lasern, *Herbstversammlung der Schweiz. Chem. Gesellschaft, Bern, 1977.*
7 H. Gugger, S. Leutwyler, E. Schumacher and G. Calzaferri, *J. Photochem.*, *9* (1978) 263.
8 M. Eigen and L. De Maeyer, in *Techniques of Chemistry*, Vol. VI, Wiley, New York, 1974.
9 H. Gugger and G. Calzaferri, *J. Photochem.*, in the press.
10 F. Erwe, *Differential- und Integralrechnung I*, B. I. Hochschultaschenbuch, 30/30a, Mannheim, 1962.